Tuning the Electrochemistry of Free-Base Porphyrins in Acidic Nonaqueous Media: Influence of Solvent, Supporting Electrolyte and Ring Substituents

Yan Cui, Lihan Zeng, Yuanyuan Fang, Jialiang M Zhu, Charles H. Devillers, Dominique Lucas, Nicolas Desbois, Claude P Gros, Karl M Kadish

Tuning the Electrochemistry of Free-Base Porphyrins in Acidic Nonaqueous Media: Influence of Solvent, Supporting Electrolyte and Ring Substituents

Yan Cui,[a] Lihan Zeng,[a] Yuanyuan Fang,[a,b] Jialiang Zhu,[a] Charles H. Devillers,[c] Dominique Lucas,[c] Nicolas Desbois,[c] Claude P. Gros,*[c] Karl M. Kadish*[a]

Abstract: A detailed study of reduction potentials, electroreduction mechanisms and acid-base chemistry was carried out on two series of free-base porphyrins in nonaqueous media. The first series is represented by four *β*-pyrrole substituted tetraphenylporphyrin (TPP) derivatives, two of which are planar and two of which are nonplanar in their non-protonated form. The second comprises porphyrins with 0-4 *meso*-phenyl groups on the macrocycle. Equilibrium constants for conversion of each neutral porphyrin to its diprotic $[H_4P]^{2+}$ form were determined and the electrochemistry was then elucidated as a function of: (i) type of nonaqueous solvent, (ii) anion of supporting electrolyte, (iii) porphyrin ring substituents and (iv) concentration of acid added to solution. Spectroelectrochemistry was used to characterize absorption spectra of each electroreduced species and, when combined with results of the above studies, improves significantly our ability to tune redox reactivity of these type compounds.

Introduction

Studies of porphyrins and porphyrin analogues have long attracted the attention of chemists, biochemists and material scientists due to their biological relevance and their use as materials in a number of applications.[1, 2] All porphyrins can be oxidized or reduced in a number of steps,[3] with the overall electrochemical behavior and redox potentials depending upon a number of factors, the most important of which are the type and oxidation state of the central metal ion, the solution conditions, the type, location and number of substituents on the porphyrin and the type and number of axial ligands in the case of derivatives with metal ions able to bind axial ligands.[4]

One key difference between the electrochemistry of free-base porphyrins and the related metalloporphyrins containing +2, +3 or +4 central metal ions is the presence of homogenous chemical reactions that follow or proceed electron transfers of the free-base derivatives and lead to irreversible redox processes on the cyclic voltammetry timescale. These chemical reactions are related, in part, to the planarity of the porphyrin macrocycle[5] and in part to the solution conditions,[3, 4] and often involve the loss or gain of protons leading to derivatives which are themselves electroactive and subject to additional coupled protonation/deprotonation reactions at the four core nitrogens, as well as proton addition to the π-ring system of the macrocycle[6-9] following electroreduction.

The four central nitrogen atoms of a free-base porphyrin are able to accept one or two additional protons to produce protonated species of the type $[H_3P]^+$ and $[H_4P]^{2+}$ [5, 10-13] and these reactions have been examined in both aqueous and non-aqueous media as well as in mixed organic-aqueous solvents.[5, 11, 14-18]

The diprotonated free-base porphyrins H_4P^{2+} can also be associated with two anions which will ion-pair to the central NH^+groups in a near-symmetrical manner above and below the plane of the porphyrin macrocycle.[18, 19] These compounds are then represented as $H_4P(X)_2$, where X = F^-, Cl^-, Br^-, I^- or PF_6^- [12, 19-22] Previous studies on interactions of diprotonated porphyrins with anions have focused in large part on structural aspects,[12, 19] the relationships between hydrogen-bond formation and the photophysical properties of the ion-paired diprotonated compounds,[23, 24]or the assembly properties of the compounds for applications in smart soft nanomaterials for data storage and processing, chiral sensing, optobioelectronics, chiroptical devices and catalysis.[17, 25-30] However, to our knowledge, there have been no systematic investigations which have focused on the interacting effects of anions, solvent and porphyrin structures on the protonation, electrochemistry and spectroscopic properties of the diprotonic free-base porphyrins during or after electroreduction in nonaqueous media.

This is investigated in the current manuscript, where the reduction potentials, electroreduction mechanisms and acid-base chemistry are examined for two related series of free-base tetraphenylporphyrins whose structures are shown in Schemes 1 and 2. The first group of compounds (Scheme 1) is represented by four *β*-pyrrole substituted TPP derivatives, two of which are planar and two of which are nonplanar in their initial non-protonated form.[31-34] The second (Scheme 2) is comprised of porphyrins with 0-4 *meso*-phenyl groups on the macrocycle.

Equilibrium constants for the conversion of each free-base derivative (represented by H_2P) to its diprotic $[H_4P]^{2+}$ form are determined in the present paper by spectroscopic methods and the electrochemistry of $[H_4P]^{2+}$ is elucidated as a function of the following four parameters: (i) type of nonaqueous solvent, (ii) type of supporting electrolyte, (iii) substituents on the porphyrin macrocycle and (iv) concentration of trifluoroacetic acid (TFA) added to solution. Special emphasis is placed on $[H_4TPP]^{2+}$ whose electrochemistry was recently reported in acidic

[a] Dr.Y. Cui, L. Zeng, Dr. Y. Fang, J. Zhu, Prof. K. M. Kadish
Department of Chemistry, University of Houston
Houston, TX 77204-5003 (USA)
Fax: (+1) 713-743-2745
E-mail: kkadish@uh.edu
[b] Dr. Y. Fang
Department of Chemistry and Chemical Engineering
Jiangsu University
Zhenjiang, Jiangsu, 212013, China
[c] Dr. C. H. Devillers, Dr. N. Desbois, Prof. D. Lucas, Prof. C. P. Gros
Université de Bourgogne, ICMUB UMR6302, CNRS
9 Avenue Alain Savary, BP 47870, 21078 Dijon Cedex (France)
E-mail: claude.gros@u-bourgogne.fr

Supporting information for this article is given via a link at the end of the document.

CH_2Cl_2containing 0.1 M tetra-*n*-butylammonium perchlorate ($TBAClO_4$)[5] and shown to deviate from that of other structurally related porphyrins under the same solution conditions.

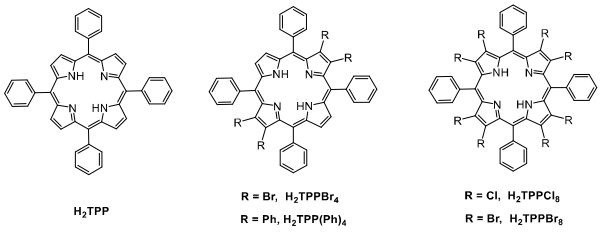

Scheme 1. Structures of investigated free-base tetraphenylporphyrin and *β*-pyrrole substituted tetraphenylporphyrin derivatives.

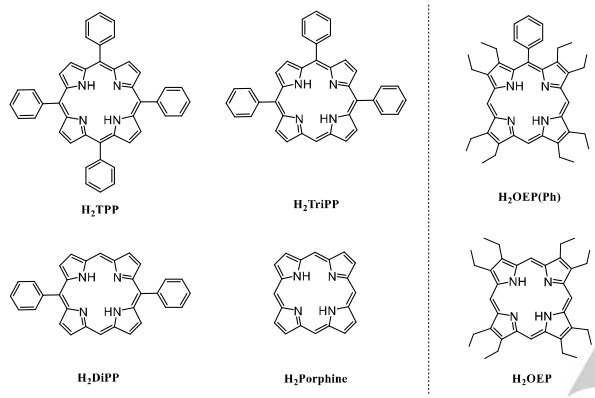

Scheme 2. Structures of free-base *meso*-phenyl substituted derivatives.

Results and Discussion

Effects of Solvent and Supporting Electrolyte on the Reductions of H_2TPP

The electroreduction of H_2TPP was investigated in four commonly used nonaqueous solvents containing different tetra-*n*-butylammonium (TBA^+) salts as supporting electrolyte. The utilized solvents were dichloromethane (CH_2Cl_2), benzonitrile (PhCN), *N,N*'-dimethylformamide (DMF) and dimethyl sulfoxide (DMSO) whose physical properties are given in Table S1. The supporting electrolytes were TBAX, where X = ClO_4^-, I^-, Br^- or Cl^-. Early studies of H_2TPP in nonaqueous media[35] had shown the presence of two stepwise one-electron transfers in solvents containing $TBAClO_4$ and this was also observed in the present study, as illustrated by the cyclic voltammograms in Figure 1.

As seen in the Figure, the ease of H_2TPP reduction follows the order CH_2Cl_2 (-1.72 V) < PhCN (-1.67 V) < DMF (-1.57 V) < DMSO (-1.48 V), which suggests an increasing stabilization of the singly-reduced porphyrin with increasing polarity of the solvent. This is indeed the case, as shown in Figure 2 which plots the first reduction potential (versus the Fc/Fc^+ couple) against two commonly used solvent parameters,[36-39] the dielectric constant, ε_r, and the Dimroth-Reichardt parameter, E_T. Both plots in Figure 2 show a linear correlation with DMSO, DMF and PhCN, but CH_2Cl_2 doesn't fit the dielectric constant plot and fits perfectly the plot of $E_{1/2}$ versus E_T, with a correlation coefficient of $R^2 = 0.995$.

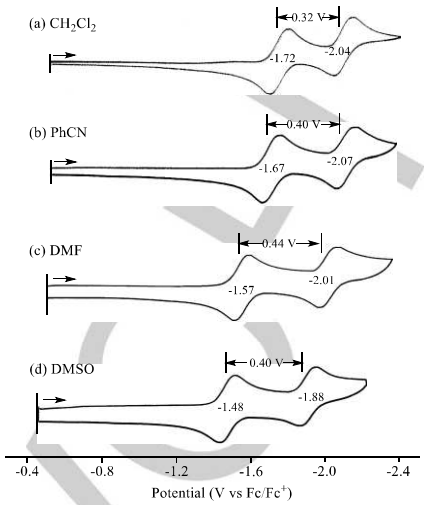

Figure 1. Effect of solvent on cyclic voltammograms of H_2TPP in (a) CH_2Cl_2, (b) PhCN, (c) DMF and (d) DMSO containing 0.1 M $TBAClO_4$. Scan rate = 0.1 V/s.

The 240 mV difference in $E_{1/2}$ between the first reduction of H_2TPP in CH_2Cl_2 (-1.72 V vs Fc/Fc^+) and DMSO (-1.48 V vs Fc/Fc^+) is consistent with a strong interaction between the solvent and the electrogenerated porphyrin π-anion radical formed after the addition of one electron but the solvent can also interact with the porphyrin in its neutral unreduced form and this can often be detected by changes in the position of absorption bands for the neutral compound prior to electroreduction. In order to examine this possibility, the spectrum of H_2TPP was measured in the four solvents with and without 0.1 M $TBAClO_4$ which was used as supporting electrolyte as well as in CH_2Cl_2 containing 0.1 M TBAX where X = Cl^-, Br^-, I^- or ClO_4^-. An example of the UV/Vis spectra of H_2TPP in CH_2Cl_2 and PhCN without supporting electrolyte is illustrated in Figure S1 and a summary of the data is given in Table 1.

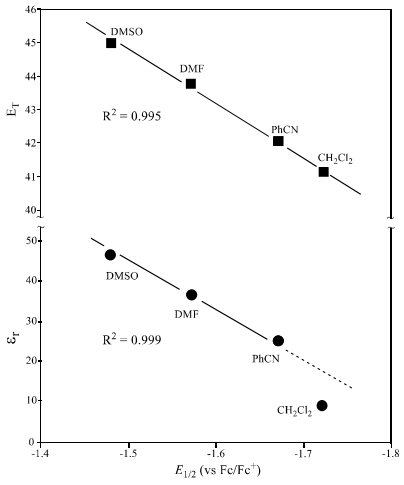

Figure 2. Plot of E_T (Dimroth-Reichardt parameter) or ε_r (dielectric constants) vs. the half wave potential (V vs Fc/Fc^+) for the first reduction of H_2TPP in CH_2Cl_2, PhCN, DMF and DMSO.

Table 1. UV/Vis spectral data (λ_{max}, nm) for neutral H_2TPP in different solvents without supporting electrolyte and in CH_2Cl_2 containing different 0.1 M TBAX salts.

Solvent	AN[a]	Anion (0.1 M)	λ /nm (logε) Soret band	Q bands			
PhCN	15.5	none	423 (5.47)	516 (4.13)	552 (3.83)	593 (3.08)	649 (3.06)
DMSO	18.8	none	420 (5.42)	515 (3.97)	549 (3.45)	591 (3.23)	646 (3.08)
DMF	16.0	none	418 (5.41)	515 (4.07)	549 (3.69)	591 (3.51)	646 (3.40)
CH_2Cl_2	20.4	none	418 (5.41)	515 (4.15)	549 (3.92)	591 (3.86)	647 (3.86)
CH_2Cl_2	20.4	TBACl	418 (5.41)	515 (4.07)	549 (3.77)	591 (3.66)	647 (3.62)
		TBABr	418 (5.40)	515 (4.34)	549 (4.19)	591 (4.12)	647 (4.06)
		TBAI	418 (5.41)	515 (4.04)	549 (3.69)	591 (3.57)	647 (3.49)
		$TBAClO_4$	418 (5.40)	515 (4.03)	549 (3.66)	591 (3.54)	647 (3.45)

[a]AN = Gutmann solvent acceptor number taken from Ref. [39]

As seen in Table 1 and Figure S1, the shape of the UV/Vis spectrum for H_2TPP is similar in each solvent, consisting of a sharp Soret band at 418-423 nm and four less intense Q bands from 515-649 nm. Several correlations were examined between the band energy (in cm^{-1}) and different solvent parameters and the best fit was found to exist between the acceptor number of the solvent (AN) and the measured wavelength of the porphyrin Soret band in CH_2Cl_2, DMSO and PhCN (but not DMF) (see Figure S2).

Anions are known to bind to the central protons of expanded free-base porphyrins and related macrocycles in their neutral form[40-47] and one of our interests in the present study was to investigate how changes in the supporting electrolyte anion would affect both the measured reduction potentials and the stability of the porphyrin products formed in the first and/or second reduction on the electrochemical and spectroelectrochemical timescale. Examples of the electrochemical data are given in Figures S3 and S4 which illustrate cyclic voltammograms of H_2TPP in the four solvents containing TBAX, where X = Cl^-, Br^-, I^- and ClO_4^-.

As seen in Figure S3, the first one-electron reduction in CH_2Cl_2 containing TBACl (-1.11 V vs. SCE) or TBABr (-1.12 V) is easier by 80-100 mV than the first one-electron reduction of the porphyrin in the same solvent containing TBAI (-1.19 V) or $TBAClO_4$ (-1.21 V). A similar trend in $E_{1/2}$ with change of supporting electrolyte is seen in DMSO (Figure S4) and, although the difference in half-wave potentials between the solution conditions is not large, the most difficult reduction in DMSO again seems to occur when using the $TBAClO_4$ salt assupporting electrolyte ($E_{1/2}$ = -1.03 V vs. SCE). More importantly, the difference in reduction half-wave potentials, when measured vs. SCE, might seem to suggest an interaction of Cl^- and Br^- with the singly reduced porphyrin in the non-bonding solvent CH_2Cl_2. However, when the reduction potentials are measured vs. the Fc/Fc^+ couple used as an internal standard, no significant differences of $E_{1/2}$ are observed with changes in the anion of the supporting electrolyte in any of the four solvents. These reduction potentials of H_2TPP vs. Fc/Fc^+ are listed in the last two columns of Table 2, and are identical to each other in all four solvents within the experimental error of the measurements (±10 mV). This lack of anion effect on the thermodynamic $E_{1/2}$ for reduction can be interpreted in terms of the four anions acting to produce an equal stabilization of the neutral and singly reduced forms of the porphyrin (according to the Nernst equation). However, an alternate interpretation is that there is no interaction at all between the supporting electrolyte anions and the neutral or singly reduced forms of the compounds which are characterized as porphyrin π-anion radicals after the addition of one electron to the conjugated macrocycle.

This latter condition seems to be the case as indicated by UV/Vis spectra of the neutral porphyrin in CH_2Cl_2 containing the four TBAX salts. The absorption bands in CH_2Cl_2 containing 0.1 M of each TBAX salt are given in Table 1 and are identical to each other, independent of the anion. The lack of an anion effect on both the UV/Vis spectrum of H_2TPP in CH_2Cl_2 and the reduction potentials of the porphyrin in CH_2Cl_2, containing 0.1 M TBAX when measured vs. Fc/Fc^+ is not what occurs for the diprotonated porphyrins $[H_4TPP]^{2+}$ in the acidic solvents and this is described in the following sections of the manuscript.

Effects of Solvent and Supporting Electrolyte on the Protonation Constants of H_2TPP and UV/Vis Spectra of $[H_4TPP]^{2+}$

The conversion of H_2TPP to its diprotonated $[H_4TPP]^{2+}$ form can be monitored by UV/Vis spectroscopy and proceeds in a single step, as written in Eq 1.[5, 12, 18, 48]

$$H_2TPP + 2H^+ \rightleftharpoons [H_4TPP]^{2+} \quad (1)$$

A $\log\beta_2$ = 9.96 was earlier reported for H_2TPP in CH_2Cl_2[5] and a smaller value of 9.10 was measured for the same reaction in the current study under the electrochemical conditions of CH_2Cl_2 containing 0.1 M $TBAClO_4$ as supporting electrolyte where the product of the titration is more correctly represented as $H_4TPP(ClO_4)_2$. Measurements of $\log\beta_2$ were also carried out for H_2TPP in CH_2Cl_2 containing the TBAI, TBABr and TBACl salts and here the final product of the titration would be represented as $H_4TPP(X)_2$, where X = I^-, Br^- or Cl^-. Examples of spectral changes monitored during these titrations are illustrated in Figure 3 and a summary of the formation constants for proton addition, $\log\beta_2$, andUV/Vis spectral data for the final ion-paired diprotic porphyrin product is given in Table 3.

Thediprotonated free-base tetraphenylporphyrin is characterized by two major absorptions, whose exact position will depend upon both the utilized solvent and the presence or absence of added TBAX. In the absence of supporting electrolyte the Soret band maxima ranges from 441-445 nm while the Q band is located at λ_{max} = 656-663 nm. There is clearly a solvent effect on the $[H_4TPP]^{2+}$ absorption spectra and there is also an effect of

anion as shown by the data in CH_2Cl_2 containing TBAX where the Soret band maximum ranges from 443-453 nm and the Q band from 659-679 nm. Despite the largedifference in the position of the peak maxima under the different solution conditions, there is no obvious trend in the positionof λ_{max} with change in the TBAX anion of the salt in solution. For example, the Soret band maximum of $[H_4TPP]^{2+}$follows the order: Br^- (453 nm) > Cl^- (449 nm) > I^- (447 nm) > ClO_4^- (441 nm), but this is not the relative order of the Q band position which ranges from 659-679 nm and follows the order: I^- (679 nm) > Br^- (671 nm) > Cl^- (666 nm) > ClO_4^- (659 nm). The Q band of $H_4TPP(I)_2$ in solutions with TBAI is not only the most red-shifted of the examined porphyrin diacids but it is also the broadest Q band with the lowest intensity. This suggests a different interaction between the I^- anions and the diprotonated form of the porphyrin, as compared to the case of $[H_4TPP]^{2+}$ in solutions with Cl^-, Br^-, or ClO_4^-. The spectrum of $H_4TPP(I)_2$ has been discussed in the literature by the groups of Rosa, Ricciardi, Baerends and Scolaro[12, 19] who examined the effects of structure and counterions on the optical properties of $H_4TPP(X)_2$, where X = F^-, Cl^-, Br^- or I^-.

The $log\beta_2$ values for protonation of H_2TPP in CH_2Cl_2 containing 0.1 M TBAX ranges from 9.10 to 9.96 and roughly correlates with the position of the Q band under the same solution conditions. This correlation is shown in Figure S5.

More significant variations in the measured $log\beta_2$ values for protonation of H_2TPP, are seen upon changing the solvent from CH_2Cl_2 to PhCN and then to DMSO or DMF. The relevant spectral changes during the titrations with TFA are illustrated in Figure S6 and the absorption maxima and measured formation constants are summarized in Table 3.

As seen in the figure and table, the spectrum of the final diprotonated porphyrin product is almost the same in the different solvents, but the values of $log\beta_2$have decreasedsubstantially in DMSO and DMF where large quantities of acid are needed to accomplish the protonation. A good correlation is seen between the $log\beta_2$ values in CH_2Cl_2, PhCN and DMSO and two solvent parameters, the dielectric constant ε_r and donor number (DN) (see Figure S7). The smallest value of $log\beta_2$ = 0.39 is obtained in DMF. This value is included in Figure S7 but does not fit the good correlation observed for other three solvents.

Effects of Solvent and Supporting Electrolyte on the Electrochemistry of $[H_4TPP]^{2+}$

The conversion of H_2TPP to its diprotonated form was electrochemically monitored during a TFA titration of the porphyrin in three different solvents (CH_2Cl_2, DMF and DMSO) containing 0.1 M $TBAClO_4$ as well as in CH_2Cl_2 containing 0.1 M of the different TBAX supporting electrolytes. Examples of the cyclic voltammograms obtained at various points of the titration

Table 2. Half-wave potentials (V vs SCE) for reduction of H_2TPP in solvents containing different supporting electrolytes at a concentration of 0.1 M.

Solvent	Dielectric Constant (ε_r)	E_T[a]	DN[b]	Electrolyte	$E_{1/2}$ (V vs SCE)		ΔE	Fc/Fc$^+$	$E_{1/2}$ (V vs Fc/Fc$^+$)	
					1st	2nd	(V)	(V)	1st	2nd
CH_2Cl_2	8.93	41.1	0.0	TBACl	-1.11	-1.43	0.32	0.62	-1.73	-2.05
				TBABr	-1.12	-1.45	0.33	0.57	-1.69	-2.02
				TBAI	-1.19	-1.51	0.32	NA	NA	NA
				$TBAClO_4$	-1.21	-1.53	0.32	0.51	-1.72	-2.04
PhCN	25.20	42	11.9	TBACl	-1.08	-1.48	0.40	0.60	-1.68	-2.08
				TBABr	-1.09	-1.49	0.40	0.58	-1.67	-2.07
				TBAI	-1.14	-1.54	0.40	NA	NA	NA
				$TBAClO_4$	-1.16	-1.56	0.40	0.58	-1.67	-2.07
DMF	36.71	43.8	26.6	TBACl	-1.06	-1.5	0.44	0.51	-1.57	-2.01
				TBABr	-1.06	-1.5	0.44	0.51	-1.57	-2.01
				TBAI	-1.07	-1.51	0.44	NA	NA	NA
				$TBAClO_4$	-1.07	-1.51	0.44	0.50	-1.57	-2.01
DMSO	46.68	45	29.8	TBACl	-0.99	-1.41	0.42	0.48	-1.47	-1.89
				TBABr	-1.00	-1.42	0.42	0.48	-1.48	-1.90
				TBAI	-1.00	-1.42	0.42	NA	NA	NA
				$TBAClO_4$	-1.03	-1.43	0.40	0.45	-1.48	-1.88

[a]E_T: Dimroth-Reichardt parameter, [b]DN = Gutmann solvent donor number taken from Ref.[39]

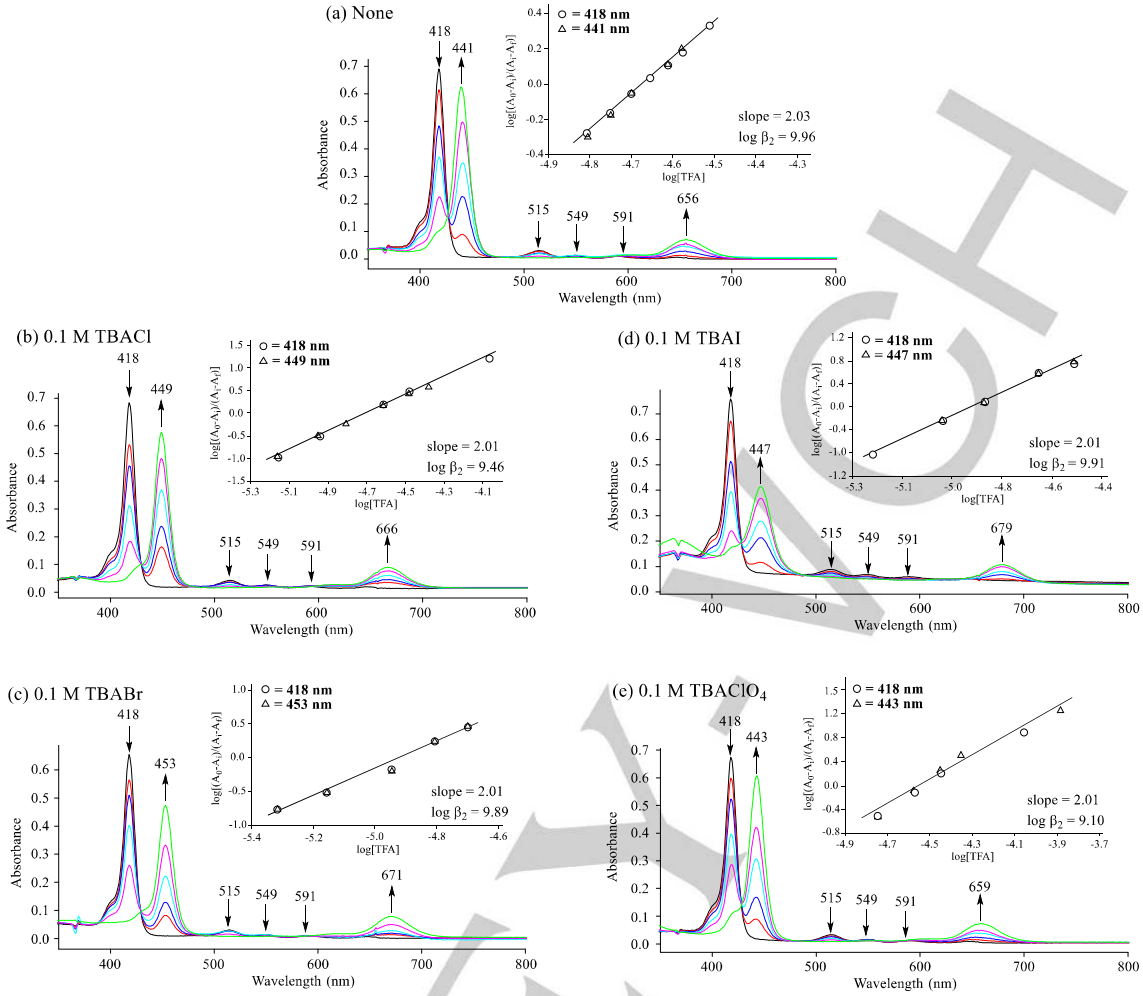

Figure 3. Effect of supporting electrolyte type on UV/Vis spectra changes of H_2TPP in CH_2Cl_2 during titration with TFA containing (a) no added salt and 0.1 M TBAX where X is (b) Cl^-, (c) Br^-, (d) I^- and (e) ClO_4^-.

Table 3. UV/Vis spectral data (λ_{max}, nm) for $H_4TPP(X)_2$ and $[H_4TPP]^{2+}$in CH_2Cl_2, PhCN and DMSO containing excess TFA and differentTBAX salts.

Solvent	Anion, X (0.1 M)	λ /nm		logβ2
		Soret band	Q band	
CH_2Cl_2	Cl^-	449	666	9.46
	Br^-	453	671	9.89
	I^-	447	679	9.91
	ClO_4^-	443	659	9.10
CH_2Cl_2	none	441	656	9.96
PhCN	none	444	664	5.86
DMSO	none	445	663	1.14
DMF	none	443	661	0.39

in CH_2Cl_2 containing 0.1 M $TBAClO_4$ are shown in Figure 4. In the absence of TFA, the initial free-base porphyrin undergoes two reversible one-electron reductions at -1.21 and -1.53 V to give a porphyrin π-anion radical and dianion, respectively. Two reduction peaks are also seen in acidic CH_2Cl_2 solutions, butunder these conditions, the first process involves an overall two electron addition to the conjugated macrocycle and the second is assigned to reduction of a product generated at the electrode surface via a chemical reaction involving the doubly reduced porphyrin as described on the following pages.

The conversion of H_2TPP to $[H_4TPP]^{2+}$ proceeds as shown in Eq. 2 and this diprotonated porphyrin species in CH_2Cl_2, 0.1 M $TBAClO_4$ is then reduced in two overlapping one-electron transfer steps at $E_p \approx$ -0.49 V (for a scan rate of 0.1 V/s) to give a transient and highly reactive doubly reduced porphyrin at the electrode surface. The reactant in Eq. 2 is represented as $[H_4TPP]^{2+}$ but mostly likely exists as $H_4TPP(ClO_4)_2$.

$$[H_4TPP]^{2+} \overset{e^-}{\rightleftharpoons} [H_4TPP]^{+} \overset{e^-}{\rightleftharpoons} [H_4TPP]^{0} \qquad (2)$$

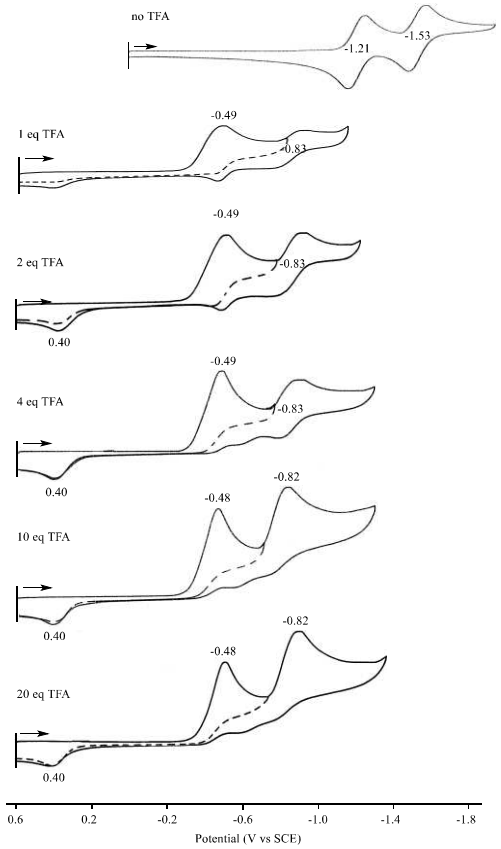

Figure 4. Cyclic voltammograms of H_2TPP (~ 10^{-4} M) in CH_2Cl_2 containing 0.1 M $TBAClO_4$ during titration with TFA. Scan rate = 0.1 V/s.

Evidence for the addition of two overlapping one-electron transfers in the first reduction of $[H_4TPP]^{2+}$ is given by comparing the peak currents for the process at $E_p \approx$ -0.49 V at different acid concentrations to the peak current for reduction of the initial compound at $E_{1/2}$ = -1.21 V in the absence of acid. This ratio of peak currents is given by i/i_0 and, when plotted vs. the [TFA]/[H_2TPP] ratio (Figure S8), clearly shows a doubling of the current for reduction of $[H_4TPP]^{2+}$ as compared to the current for reduction of H_2TPP. This is consistent with two overlapping one electron transfers at the same potential (an electrochemical EE mechanism) as opposed to a single step, two electron transfer where the current for reduction of $[H_4TPP]^{2+}$ would be proportional to $n^{3/2}$ and would thus be 2.83 times higher for $[H_4TPP]^{2+}$ than for H_2TPP.[49]

There is no change in the number of protons on the central nitrogen atoms of $[H_4TPP]^{2+}$ during the timescale of the first overall two electron reduction of this compound in CH_2Cl_2, 0.1 M $TBAClO_4$, as evidenced by the fact that the peak potential remained invariant as the acid concentration in solution was increased from 1 to 20 equivalents TFA (see Figure 4). This would not be the case if a gain or loss of protons were to occur on the electrochemical timescale where the peak potential might then be expected to shift by 60 or 120 mV for each tenfold change in $[H^+]$.[49]

As indicated above, the first reduction of $[H_4TPP]^{2+}$, at = -0.49 V in the acidic CH_2Cl_2 solution, corresponds to an overall two-electron reduction of the conjugated macrocycle and the second process at = -0.83 V in Figure 4 corresponds to the electroreduction of a phlorin anion which is generated at the electrode surface after reaction of the electrogenerated porphyrin dianion with protons in the solution. The current-voltage curves for reduction of $[H_4TPP]^{2+}$ in the acidic CH_2Cl_2 solutions of Figure 4 are similar to CV data described by Wilson and Peychal-Heiling for the reduction of H_2TPP in DMF containing 0.1 M TEAP[6] and the proposed mechanism is given in Scheme 3 where the second reversible reduction at $E_{1/2}$ = -0.83 V and first irreversible reoxidation at E_p = 0.40 V are both attributed to electrode reactions of a protonated phlorin anion which is generated at the electrode surface after formation of the doubly reduced $[H_4TPP]^0$ dianion.

The effect of the TBAX supporting electrolyte on the electrochemistry of $[H_4TPP]^{2+}$ (or $H_4TPP(X)_2$) is shown in Figure 5 which compares cyclic voltammograms of 10^{-4} M H_2TPP in CH_2Cl_2 solutions containing 4.0 equivalents of TFA and 0.1 M TBAX. The voltammograms recorded with TBACl, TBAI or TBABr as supporting electrolyte are similar to those recorded in solutions with $TBAClO_4$ in that each diprotic porphyrin undergoes an initial two-electron reduction followed by formation of an electroactive phlorin anion at the surface of the electrode. The homogenously generated phlorin anion can then be reversibly reduced by one electron at$E_{1/2}$ values of -0.76 to -0.83 V (see dashed lines in Figure 5) or it can be irreversibly reoxidized at a peak potential of 0.26 to 0.40 V (for a scan rate of 0.1 V/s) to give back the initial compound.

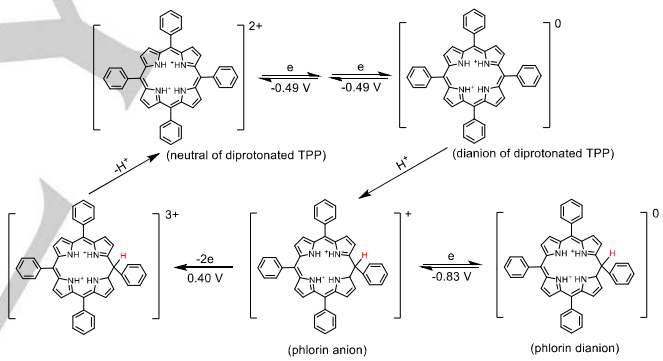

Scheme 3. Proposed mechanism for reduction of $[H_4TPP]^{2+}$ in CH_2Cl_2 containing 0.1 M $TBAClO_4$. The listed potentials are taken from voltammograms in Figure 4.

The most significant difference in redox behavior of the four $H_4TPP(X)_2$ complexes in CH_2Cl_2containing 0.1 M TBAX is that half-wave potentials for the first two one-electron additions are overlapped in potential when using $TBAClO_4$ as the supporting electrolyte but separated by 120-130 mV in the CH_2Cl_2 solutions containing 0.1 M TBACl or TBABr (Figure 5). This separation in potential leads to a reversible first reduction in the solutions with Cl^- or Br^- since the chemical reaction leading to formation of the phlorin anion is only observed after the addition of a second electron to the porphyrin conjugated π-ring system. The two reductions of H_2TPP in CH_2Cl_2 containing TBAI are also separated in potential by about 100 mV and a quasi-reversible first reduction is observed at $E_{1/2}$ = -0.43 V. However, formation of the phlorin anion is rapid after the second electron addition in the TBAI solution and a totally reversible initial reduction of the porphyrin cannot be observed under these solution conditions.

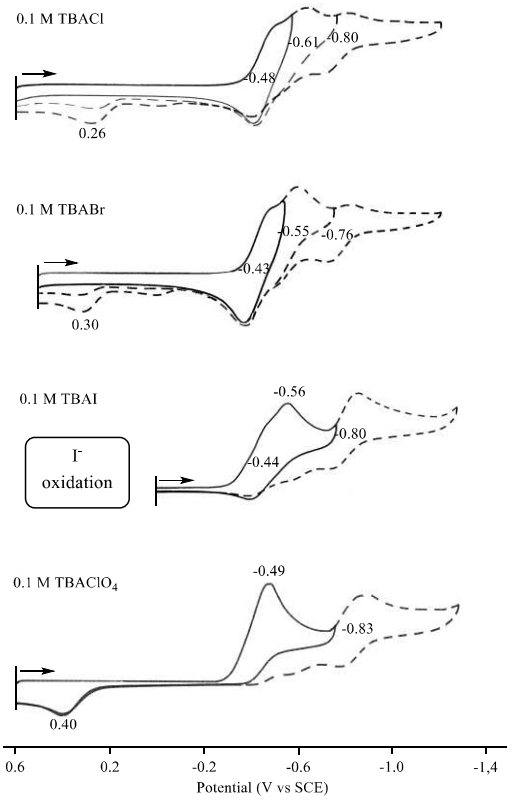

Figure 5. Cyclic voltammograms of H_2TPP (~10^{-4} M) in CH_2Cl_2 containing 4 eq TFA and 0.1 M TBACl, TBABr, TBAI and $TBAClO_4$ different supporting electrolytes.

A splitting of the two overlapping redox reactions of $H_2TPP(X)_2$ into two well resolved one-electron transfer processes occurs not only in solutions of CH_2Cl_2 containing Cl^-, Br^-, and in part I^- ,but also in DMF containing high acid concentrations and 0.1 M ClO_4^- from the $TBAClO_4$ supporting electrolyte. This is illustrated in Figure S9 where the first two one-electron reductions of 10^{-4} M H_2TPP in DMF, 0.1 M $TBAClO_4$ are overlapped in potential in solutions containing up to 20 eq TFA but begin to separate from each other as the acid concentration is increased from 100 to 1000 eq TFA (corresponding to 0.01 to 0.1 M TFA concentration).

The first one electron reduction occurs at progressively more positive potentials with increase in the acid concentration while the second electron addition occurs at an $E_{1/2}$ value which is independent of the acid concentration after 20 eq TFA have been added to the solution.

Two points should be noted with respect to the electrochemical data in Figure S9. The first is that the facile redox process at low TFA concentrations occurs under the application of an applied reducing potential which converts the unprotonated H_2TPP species in the bulk of the DMF solution to its more easily reducible diprotic form, $[H_4TPP]^{2+}$. The bulk conversion of H_2TPP which is reduced at -1.07 V to $[H_4TPP]^{2+}$ which is reduced at -0.40 V requires large quantities of TFA as indicated by the measured $\log\beta_2$ value of 0.39 in the DMF solvent. (Figure S6). However, the rate of conversion of H_2TPP to $[H_4TPP]^{2+}$ is extremely rapid and this facilitates a shifting of the equilibrium towards the more easily reducible species as shown in Scheme 4.

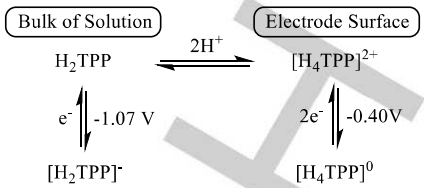

Scheme 4. Equilibrium between H_2TPP and more easily reducible $[H_4TPP]^{2+}$ in the presence of an applied reducing potential.

Effect of Macrocycle Structure on Reduction of Free-base *β*-Pyrrole Porphyrin Diacids

A recent publication from our laboratory described the electrochemistry for a series of planar and non-planar *β*-pyrrole substituted free-base porphyrins in CH_2Cl_2 containing 0.1 M $TBAClO_4$ and added acid in the form of TFA[5] andfour of the porphyrins from this earlier investigation are now further characterized in the present study when dissolved in acidic CH_2Cl_2 solutions containing TBACl, TBABr or TBAI as supporting electrolyte instead of $TBAClO_4$.

The structures of the investigated *β*-pyrrole substituted porphyrins are shown in Scheme 1 where the planar porphyrins are represented by H_2TPPBr_4 and $H_2TPP(Ph)_4$ and the non-planar porphyrins by H_2TPPBr_8 and H_2TPPCl_8. The planar porphyrins were earlier shown to exhibit two well-defined one-electron reductions in CH_2Cl_2 containing 0.1 M $TBAClO_4$, while the nonplanar porphyrins exhibited complex redox behavior and coupled chemical reactions under the same solution conditions.[5] In each case, however, when acid in the form of TFA was added to the CH_2Cl_2 solution, the porphyrin electrochemistry was then characterized by a reversible and facile two-electron reduction at low TFA concentrations and an irreversible or quasi-irreversible facile two-electron reduction at higher concentrations of TFA.

Examples of this behavior for two of the porphyrins, $H_2TPP(Ph)_4$, which is planar, and H_2TPPCl_8, which is nonplanar, are shown by the cyclic voltammograms in Figure 6. Both compounds exhibit a reversible two-electron transfer in CH_2Cl_2 containing 0.1 M $TBAClO_4$ and 1.5-2.0 equivalents TFA.

The crossover between a reversible two-electron reduction in CH_2Cl_2 containing low acid concentration to an irreversible two-electron reduction at higher concentrations of acid (such as that illustrated in Figure 6a) is related to reaction of the doubly reduced porphyrin and formation of a protonated phlorin anion but it was not clear if changing the solvent or the supporting anion from the weakly coordinating ClO_4^- to the more strongly coordinating Cl^-, Br^- or I^- would lead to a stabilization of the singly reduced *β*-pyrrole substituted porphyrin. It was also not clear if changes in the solvent or supporting electrolyte anion would lead to a separation of the two overlapping one-electron transfer steps into two separate one-electron transfer redox processes as also occurs for H_2TPP and described in earlier sections of this manuscript.

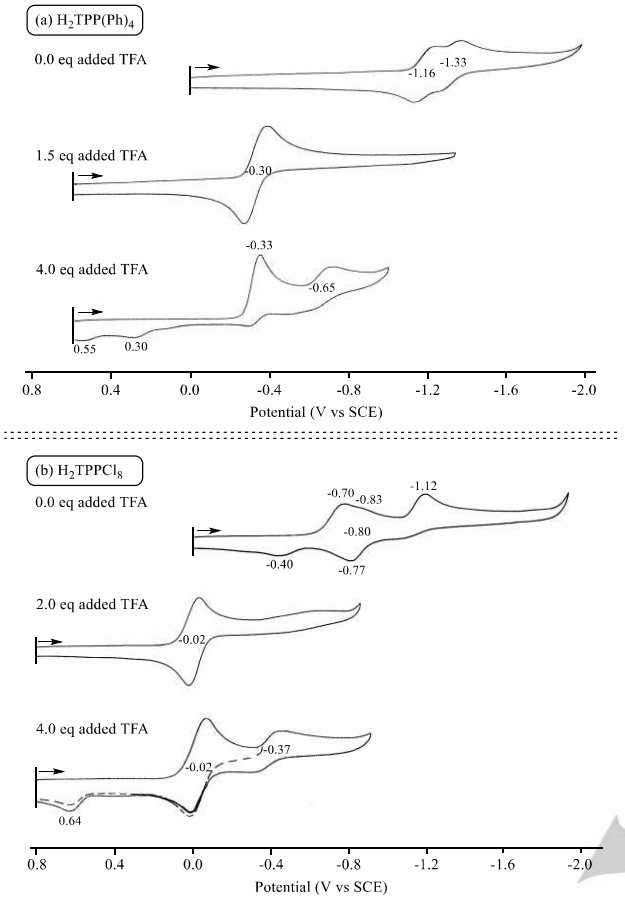

Figure 6. Comparison of cyclic voltammograms for (a) planar $H_2TPP(Ph)_4$ and (b) nonplanar H_2TPPCl_8 in CH_2Cl_2 containing 0.1 M $TBAClO_4$ and different concentrations of added TFA. Scan rate = 0.1 V/s.

The answer to this question is clear cut and shown by the cyclic voltammograms in Figure 7 for H_4TPPCl_8 in CH_2Cl_2 before and after the addition of 2 eq TFA to solutions containing the four TBAX supporting electrolytes, where X = Cl^-, Br^-, I^- or ClO_4^-. Under all four solution conditions there is a minimum amount of phlorin anion formation after the addition of acid as evidenced by the reversible redox processes and the lack of a major reduction peak following formation of the doubly reduced species. The two one-electron additions to the porphyrin π-ring system are overlapped in potential and located at $E_{1/2}$ = -0.01 V in the CH_2Cl_2 solutions containing 0.1 M $TBAClO_4$ and 2.0 eq TFA but two well-separated one-electron transfers are seen in the CH_2Cl_2/TFA solutions containing TBACl, TBABr, or TBAI as supporting electrolyte. The first one-electron reduction of H_4TPPCl_8 is located at $E_{1/2}$ = -0.01 to 0.02 V under all four solution conditions, while the half-wave potential for the second one-electron addition varies with the strength of the anion and is located at $E_{1/2}$ values of -0.18, -0.13 or -0.12 V in CH_2Cl_2 solutions containing respectively, TBACl, TBABr or TBAI (Figure 7b). The electrode reactions under these conditions are proposed to occur as shown in Eqs 3 and 4 where all three forms of the diacid are written as being ion paired with the anion of the supporting electrolyte on the electrochemical timescale.

$$H_4P(X)_2 + e^- \rightleftharpoons [H_4P(X)_2]^- \quad (3)$$

$$[H_4P(X)_2]^- + e^- \rightleftharpoons [H_4P(X)_2]^{2-} \quad (4)$$

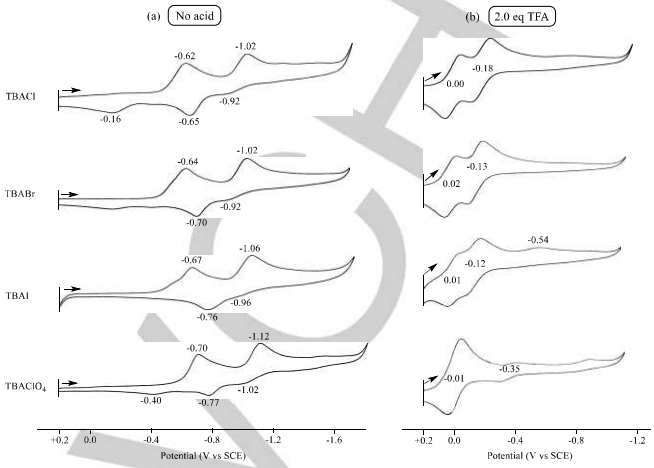

Figure 7. Cyclic voltammograms of H_2TPPCl_8 in (a) CH_2Cl_2 containing different 0.1 M TBAX supporting electrolytes where X= Cl^-, Br^-, I^- and ClO_4^- and (b) after adding 2.0 eq TFA to the solution. Scan rate = 0.1 V/s.

The difference in potential between the first and second one-electron reductions of $H_4TPPCl_8(X)_2$ increases with increasing strength of the supporting electrolyte anion and in CH_2Cl_2 containing 2.0 eq TFA the $\Delta E_{1/2}$ follows the order: ClO_4^- (0 mV) < I^- (130 mV) < Br^- (150 mV) < Cl^- (180 mV). A similar trend of $\Delta E_{1/2}$ with change in the anion of the supporting electrolyte is also seen for the octabromoporphyrin $H_4TPPBr_8(X)_2$ in CH_2Cl_2 containing 2.0 eq TFA and the same four 0.1 M TBAX supporting electrolytes. Also, like in the case of $H_4TPPCl_8(X)_2$ (Figure 7), the potential separation between the two one-electron reductions at the porphyrin macrocycle is equal to zero when using $TBAClO_4$ as supporting electrolyte and this process is then characterized by two overlapping one electron transfers at the same potential of -0.02 V vs SCE.A summary of the measured values of $E_{1/2}$ and $\Delta E_{1/2}$ value is given in Table S2 for the four examined β-pyrrole substituted porphyrins in acidic CH_2Cl_2 solutions containing 0.1 M TBAX, where X = Cl^-, Br^-, I^- and ClO_4^-.

Thin-layer UV/Vis Spectroelectrochemistry.

As previously described in the literature,[5] a spectroelectrochemical monitoring of the reduction of $[H_4TPP]^{2+}$, $[H_4TPP(Ph)_4]^{2+}$ or $[H_4TPP(Br)_4]^{2+}$ in CH_2Cl_2 solutions containing 2.0 equivalents TFA led to a UV/Vis spectrum with absorption bands which were exactly the same as that for the neutral unreduced and unprotonated porphyrins in CH_2Cl_2. However, as shown in the present study, different UV/Vis spectra are obtained after reduction of the same diprotic porphyrins in CH_2Cl_2 containing 0.1 M TBAP and higher concentrations of TFA (10 to 20 equivalents). Examples of the spectral changes obtained under these conditions are shown in Figures 8a-c for $[H_4TPP]^{2+}$, $[H_4TPP(Ph)_4]^{2+}$ and $[H_4TPP(Br)_4]^{2+}$, respectively.

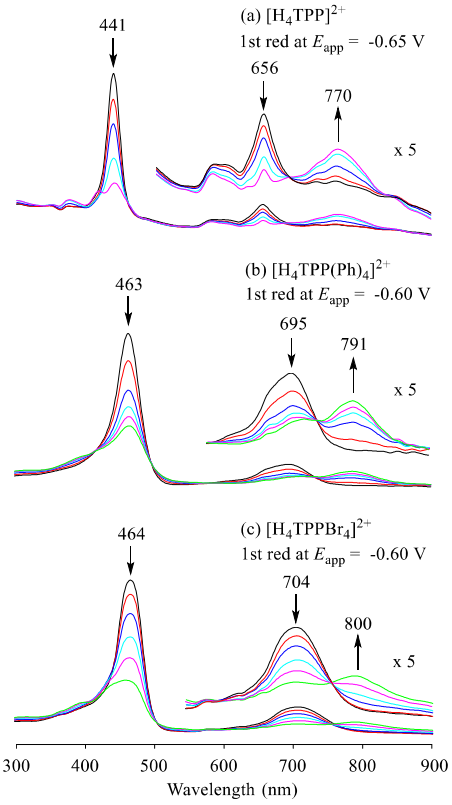

Figure 8. Thin-layer UV/Vis spectra changes of (a) $[H_4TPP]^{2+}$, (b) $[H_4TPP(Ph)_4]^{2+}$ and (c) $[H_4TPPBr_4]^{2+}$ during the first controlled reduction potential in CH_2Cl_2containing 10-20 eq TFA and 0.1 M $TBAClO_4$.

The initial UV/Vis spectrum of the diprotonated compound is characterized by a Soret band at 441-464 nm and a broad Q band at 656-704 nm. As the reduction proceeds, the Soret band absorption decreases significantly in intensity and a new intense Q band appears at 770-800 nm. Isosbestic points are observed for all three sets of spectral changes and the final spectrum of the reduced product, with bands at 770-800 nm, is again assigned to a phlorin anion. These spectra are similar to UV/Vis spectra reported in the literature for the phlorin anions of related porphyrins.[6-9]

A different type of spectral change is seen upon reduction of the diprotonated octabromo- and octachloroporphyrins in CH_2Cl_2 solutions with excess TFA (in this case 20 equivalents). Examples of these spectral changes are shown in Figure 9. The initial UV/Vis spectrum of the unreduced porphyrins under these conditions is characterized by a Soret band at 484 or 494 nm and a Q band at 730 or 745 nm, all of which are red shifted as compared with bands for unreduced $[H_4TPP]^{2+}$, $[H_4TPP(Ph)_4]^{2+}$ and $[H_4TPPBr_4]^{2+}$ whose spectra are shown in Figure 8.

The bleaching of the Soret band and the formation of a strong near-IR band at 770-800 nm upon the two electron reduction of the diprotic porphyrins in Figure 8 is consistent with generation of a phlorin anion in solution but these types of spectral changes are not seen in Figure 9 where the product of the two-electron reduction has a much decreased intensity Soret band and a broad near-IR band from 800-1000 nm. This is strong evidence for the lack of a phlorin anion being generated upon reduction of $[H_4TPPCl_8]^{2+}$ or $[H_4TPPBr_8]^{2+}$ on the thin-layer spectroelectrochemical timescale.

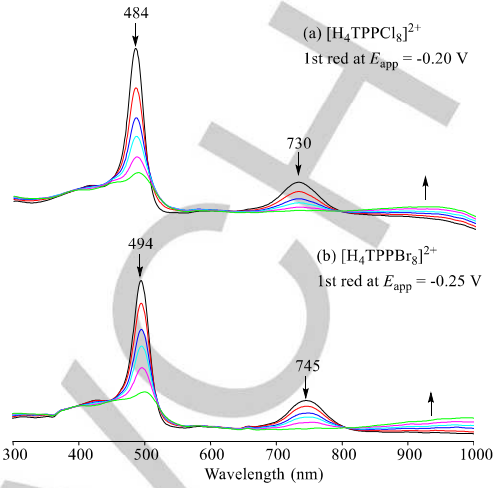

Figure 9. Thin-layer UV/Vis spectra changes of (a) $[H_4TPPCl_8]^{2+}$ and (b) $[H_4TPPBr_8]^{2+}$ during the first controlled potential reduction in CH_2Cl_2, containing 0.1 M $TBAClO_4$ and 20 eq TFA

Effect of *Meso*-Substitution on the UV/Vis Spectra of Neutral and Protonated Porphyrins

In this section, we describe the electrochemistry, UV/Vis spectra and acid-base properties of porphyrins with zero, two, three and four *meso*-phenyl substituents on the macrocycle. Structures of this series of compounds are given in Scheme 2 and their UV/Vis spectra in CH_2Cl_2 are given by Table 4. As seen from Table 4, the Soret band of each compound is systematically red shifted from 392 to 418 nm when increasing the number of *meso*-phenyl substituents from 0 to 4 and a similar red shift is seen in the four Q bands which are located at 488, 519, 562 and 612 nm for the free-base porphine and 515, 549, 591 and 647 nm for H_2TPP in CH_2Cl_2. A plot of the Soret band wavelength vs the number of *meso*-phenyl groups on the porphyrin is given by Figure 10 and shows a linear relationship with a correlation coefficient of 0.997.

The compounds in Table 4 were also spectrally monitored during conversion to their diprotic form during a titration with TFA in CH_2Cl_2. Examples of the resulting spectral changes upon conversion of the neutral porphyrin to its diprotic form are given in Figures 11 and 12 for H_2TriPP, H_2DiPP and $H_2Porphine$ and a summary of the spectral data for the final diprotic porphyrin product is given in Table 5 which also includes the measured $\log\beta_2$ values in CH_2Cl_2.

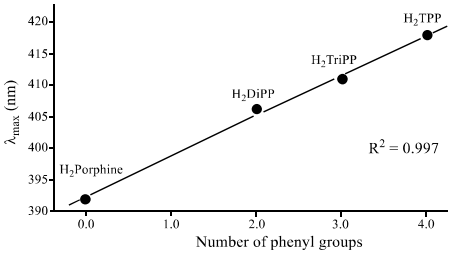

Figure 10. Plot of Soret band wavelength of the investigated porphyrins vs. number of *meso*-phenyl groups.

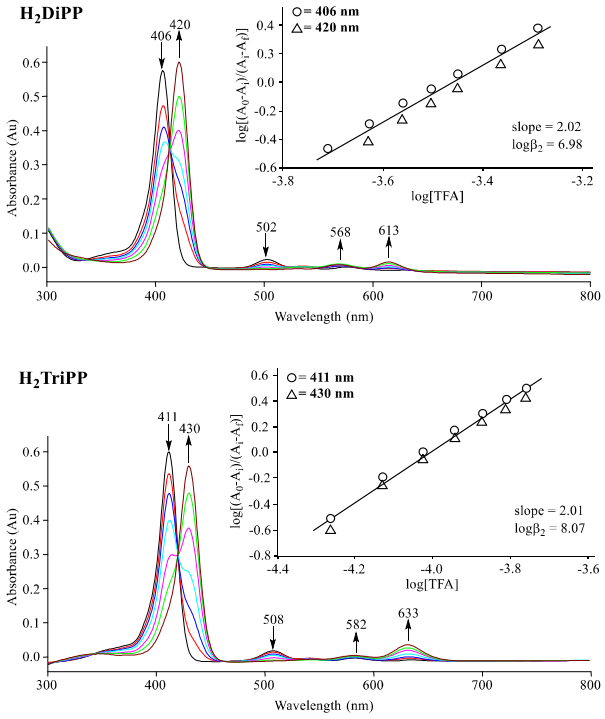

Figure 11. UV/Vis spectral changes during the protonation of H_2DiPP and H_2TriPP with TFA in CH_2Cl_2. The figure inset shows the Hill plot used to analyze the data.

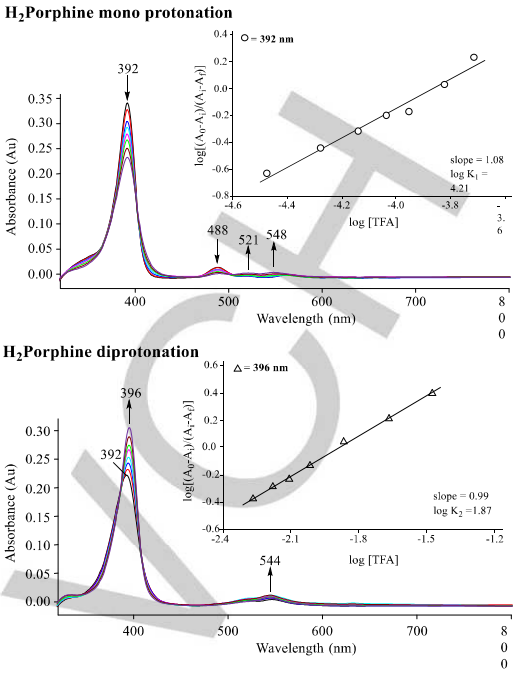

Figure 12. UV/Vis spectral changes during the first and second protonations of H_2Porphine with TFA in CH_2Cl_2. The figure inset shows the Hill plot used to analyze the data.

Like in the case of the neutral porphyrins of Scheme 2, there is a systematic red shift in the position of both the Soret band and the most intense Q band in the spectrum of the diprotic porphyrins upon increasing the number of *meso*-phenyl groups from 0 to 4, and a plot of λ_{max} vs the number of phenyl groups on the compound is again linear as shown in Figure 13.

A plot of $\log\beta_2$ vs the number of phenyl groups on the porphyrin is also linear for the *meso*-substituted compounds with 2, 3 or 4 phenyl groups but H_2Porphine (the compound with zero *meso*-phenyl groups) does not fit this plot and proton addition to the central nitrogen atoms of the macrocycle occurs in two separate steps, with measured formation constants of $\log K_1$ = 4.21 and $\log K_2$ = 1.87.

Table 4. UV/Vis spectral data for investigated *meso*-phenyl substituted porphyrins in CH_2Cl_2.

# of *meso*-phenyl	Compound	λ/nm				
		Soret	Q bands			
0	H_2Porphine	392	488	519	562	612
2	H_2DiPP	406	502	534	576	632
3	H_2TriPP	411	508	541	583	638
4	H_2TPP	418	515	549	591	647
0	H_2OEP	398	499	531	666	619
1	H_2OEP(Ph)	404	503	537	572	625

A similar stepwise protonation with formation of $[H_3OEP]^+$ has earlier been reported for H_2OEP[50] and this was confirmed in the present study which measured the binding constants in CH_2Cl_2. The relevant data are shown in Figure S10 where $\log K_1$ = 5.18 and $\log K_2$ = 2.93.

The stepwise conversion of neutral H_2Porphine and H_2OEP to their monoprotic and diprotic forms (Figures 12 and S10) differs from that of the other investigated *meso*-phenyl substituted compounds examined in this study where a simultaneous addition of two protons to the neutral porphyrin was observed in all cases. It was therefore of interest to know what would occur for a porphyrin containing a single *meso*-phenyl substituent and only protons at the other *meso*- and *β*-pyrrole positions of the macrocycle. Unfortunately, this porphyrin was not available for study and the closest comparison compound is given by H_2OEP(Ph) whose structure is shown in Scheme 2.

Table 5. UV/Vis spectral data of diprotonated porphyrins and protonation constants for the investigated *meso*-phenyl substituted porphyrins in CH_2Cl_2.

# of *meso*-phenyl	Compound	λ/nm		n	$\log\beta_2$
		Soret	Q		
0	$[H_4Porphine]^{2+}$ [a]	396	544	2.07	6.08
2	$[H_4DiPP]^{2+}$	420	613	2.02	6.98
3	$[H_4TriPP]^{2+}$	430	633	2.01	8.07
4	$[H_4TPP]^{2+}$	441	656	2.03	9.96
0	$[H_4OEP]^{2+}$ [b]	403	547	2.01	8.11
1	$[H_4OEP(Ph)]^{2+}$	422	572	2.02	10.39

[a]H_2Porphine can be protonated by two steps with $\log K_1$ = 4.21 (n = 1.08) and $\log K_2$ = 1.87 (n = 0.99). Thus $\log\beta_2$ = 6.08. [b]The protonation of H_2OEP occurs in two steps with $\log K_1$ = 5.18. (n = 1.00) and $\log K_2$ = 2.93 (n = 1.01). Thus $\log\beta_2$ = 8.11.

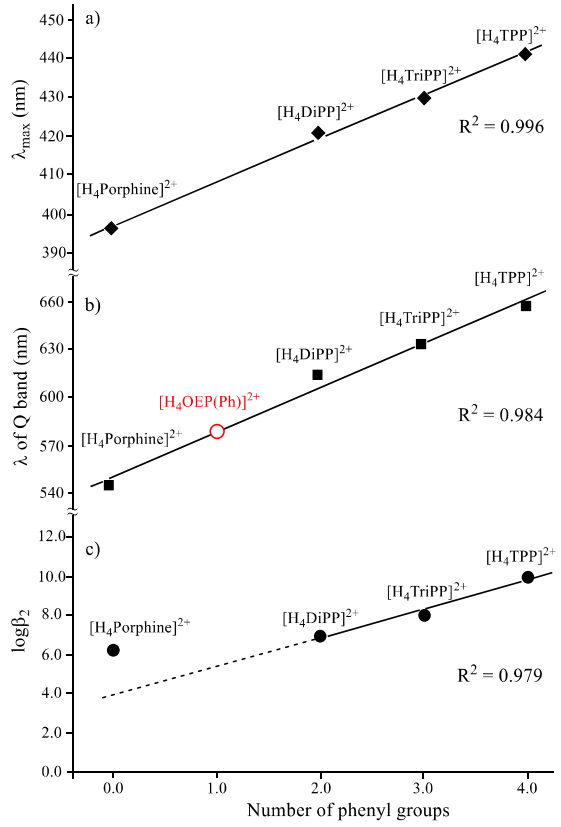

Figure 13. Correlation of a) λ_{max} (nm) of UV/Vis spectrum, b) wavelength Q band (nm) and c) the diacid formation constant logβ_2 of *meso*-phenyl substituted porphyrins vs. the number of *meso*-phenyl substituents on macrocycle. The data were obtained in CH_2Cl_2 containing excess TFA.

Surprisingly, the conversion of H_2OEP(Ph) to $[H_4OEP(Ph)]^{2+}$ was extremely facile and occurred in a single two-proton addition step with a logβ_2 = 10.39. These spectral changes are shown in Figure S11 where the spectrum of the diprotonated porphyrin is characterized by an intense Soret band at 422 nm and a single Q band at 572 nm. These values are listed in Table 5. Neither the Soret band wavelength nor the calculated logβ_2 value for H_2OEP(Ph) fit correlations between this parameter and the number of *meso*-phenyl groups on the macrocycle shown in Figure 13 but the wavelength of the Q band does fit a correlation vs the number of *meso*-phenyl groups and this data point is included in Figure 13b for the correlation involving the Q band position.

Experimental Section

Chemicals: Absolute dichloromethane (CH_2Cl_2, 99.8%) from EMD Chemicals Inc. was used for electrochemistry without further purification. Benzonitrile (PhCN) was purchased from Sigma-Aldrich Chemical Co. and distilled over P_2O_5 under vacuum prior to use. N,N'-dimethylformamide (DMF) and dimethyl sulfoxide (DMSO) were purchased from Sigma-Aldrich Chemical Co.. Tetra-*n*-butylammonium perchlorate ($TBAClO_4$), tetra-*n*-butylammonium chloride > 97% (TBACl), tetra-*n*-butylammonium bromide > 98% (TBABr) and tetra-*n*-butylammonium iodide > 99% (TBAI), used as supporting electrolyte, were purchased from Sigma-Aldrich, recrystallized from ethyl alcohol, and dried under vacuum at 40 °C for at least one week prior to use. Trifluoroacetic Acid (TFA) > 99% was purchased from Sigma-Aldrich Chemical Co..

5,10,15,20-tetraphenylporphyrin, 5,10,15,20-tetra(4-pyridyl)porphyrin, 5,15-diphenylporphyrin and 5,10,15-triphenylporphyrin were purchased from PorphyChem in Dijon, France. The *β*-pyrrole substituted free-base porphyrins in Chart 1[46,51-53] and the free-base porphine in Chart 2[54, 55] were synthesized using literature procedures.

Instrumentation: Cyclic voltammetry was carried out with an EG&G model 173 potentiostat/galvanostat. A homemade three-electrode electrochemistry cell was used, consisting of a platinum button or glassy carbon working electrode (diameter = 0.3 mm), a platinum wire counter electrode, and a saturated calomel reference electrode (SCE). The SCE was separated from the bulk of the solution by a fritted-glass bridge of low porosity, which contained the solvent/supporting electrolyte mixture. Potentials are referenced to the SCE.

Spectroscopically monitored titrations with acid or base were carried out in a home-built 1.0 cm cell. Thin-layer UV-visible spectroelectrochemical experiments were also carried out with a home-build cell that has a light transparent platinum net working electrode and a cell path length of about 1.0 mm.[56] Potentials were applied and monitored with an EG&G PAR Model 173 potentiostat. Time-resolved UV-visible spectra were recorded with a Hewlett-Packard Model 8453 diode array spectrophotometer. High purity N_2 from Trigas was used to deoxygenate the solution and was kept over the solution during each electrochemical and spectroscopic experiment.

Determination of Formation Constants: The changes in UV-visible spectra for each investigated free-base porphyrin in CH_2Cl_2 were monitored during a titration with trifluoroacetic acid (TFA) and the resulting spectral data then used to calculate the formation constants for proton addition by using the Hill equation[57, 58] (Eq. 5)

$$\log[(A_0-A_i)/(A_i-A_f)] = \log K + n\log[H^+] \quad (5)$$

where A_0 = the initial absorbance in which $[H^+]$ = 0.0, A_f = the final absorbance of the fully protonated porphyrin and A_i = the absorbance at a given proton concentration during the titration. The slope of the $\log[(A_0-A_i)/(A_i-A_f)]$ versus $\log[H^+]$ plot gives n, the number of protons added to the core nitrogen atoms (or the pyridyl groups in the case of the pyridylporphyrins). The value of logK (or logβ_2 in most cases) was then calculated from the intercept of the line at $\log[(A_0-A_i)/(A_i-A_f)]$ = 0.0. In the present study, the logK_2 and logβ_2 values were evaluated by using a minimum of two wavelengths, and an average value of n and log of the formation constant is reported.

Acknowledgements

Support was provided by the Robert A. Welch Foundation (KMK, Grant E-680), Natural Science Foundation of China (Grant No. 21501070), the CNRS France (UMR 6302), the "*Université de Bourgogne*" and the "*Conseil Régional deBourgogne*" through the 3MIM-integrated project ("*Marquage deMolécules par les Métaux pour l'Imagerie* Médicale"). The French Ministry of Research is also acknowledged for PhD scholarship. C.H.D.

thanks the CNRS for granting him the opportunity to work as a full-time researcher for one year ("délégation CNRS", Sept. 2015). We are thankful to Dr. Hai-Jun Xu and Dr. Yi Chang for the preparation of some porphyrin derivatives. We are very thankful to Dr. Benoit Habermeyer and Porphychem Co. for providing some porphyrin precursors.

Keywords:electrochemistry•free-base porphyrin•protonation• spectroelectrochemistry• supporting electrolyte

[1] In *The Porphyrin Handbook, Vol. 1-20* (Eds.: K. M. Kadish, K. M. Smith, R. Guilard), Academic Press, New York, **2000 and 2003**.
[2] In *Handbook of Porphyrin Science, Vol. 1-35* (Eds.: K. M. Kadish, K. M. Smith, R. Guilard), World Scientific, Singapore, **2010-2014**.
[3] K. M. Kadish, in *Progress in Inorganic Chemistry, Vol. 34* (Eds.: S. J. Lippard), John Wiley & Sons, Inc. , New York, **1986**, pp. 435-606.
[4] K. M. Kadish, Smith, K. M., Guilard, R., *Vol. 8* (Eds.: K. M. Kadish, Van Caemelbecke, E., Royal, G.), Academic Press, New York, **2000**, pp. 1 - 114.
[5] Y. Fang, P. Bhyrappa, Z. Ou, K. M. Kadish, *Chem. - Eur. J.* **2014**, *20*, 524-532.
[6] G. S. Wilson, G. Peychal-Heiling, *Anal. Chem.* **1971**, *43*, 550-556.
[7] G. S. Wilson, G. Peychal-Heiling, *Anal. Chem.* **1971**, *43*, 545-550.
[8] J. G. Lanese, G. S. Wilson, *J. Electrochem. Soc.* **1972**, *119*, 1039-1043.
[9] Y. Fang, Y. G. Gorbunova, P. Chen, X. Jiang, M. Manowong, A. A. Sinelshchikova, Y. Y. Enakieva, A. G. Martynov, A. Y. Tsivadze, A. Bessmertnykh-Lemeune, C. Stern, R. Guilard, K. M. Kadish, *Inorg. Chem.* **2015**, *54*, 3501-3512.
[10] Z. Samec, J. Langmaier, A. Trojanek, S. Zalis*, Vol. 34*, World Scientific Publishing Co. Pte. Ltd., **2014**, pp. 97-146.
[11] B. Su, F. Li, R. Partovi-Nia, C. Gros, J.-M. Barbe, Z. Samec, H. H. Girault, *Chem. Commun. (Cambridge, U. K.)* **2008**, 5037-5038.
[12] G. De Luca, A. Romeo, L. M. Scolaro, G. Ricciardi, A. Rosa, *Inorg. Chem.* **2007**, *46*, 5979-5988.
[13] S. Thyagarajan, T. Leiding, S. P. Arskold, A. V. Cheprakov, S. A. Vinogradov, *Inorg. Chem.* **2010**, *49*, 9909-9920.
[14] O. Finikova, A. Galkin, V. Rozhkov, M. Cordero, C. Haegerhaell, S. Vinogradov, *J. Am. Chem. Soc.* **2003**, *125*, 4882-4893.
[15] A. Stone, E. B. Fleischer, *J. Amer. Chem. Soc.* **1968**, *90*, 2735-2748.
[16] D. K. Maity, R. L. Bell, T. N. Truong, *J. Am. Chem. Soc.* **2000**, *122*, 897-906.
[17] A. V. Udal'tsov, L. A. Kazarin, A. A. Sweshnikov, *J. Mol. Struct.* **2001**, *562*, 227-239.
[18] Y. Zhang, M. X. Li, M. Y. Lue, R. H. Yang, F. Liu, K. A. Li, *J. Phys. Chem. A* **2005**, *109*, 7442-7448.
[19] A. Rosa, G. Ricciardi, E. J. Baerends, A. Romeo, L. M. Scolaro, *J. Phys. Chem. A* **2003**, *107*, 11468-11482.
[20] S. Y. Ma, *Chem. Phys. Lett.* **2000**, *332*, 603-610.
[21] D.-M. Chen, X. Liu, T.-J. He, F.-C. Liu, *Chem. Phys.* **2003**, *289*, 397-407.
[22] A. Rosa, G. Ricciardi, E. J. Baerends, *J. Phys. Chem. A* **2006**, *110*, 5180-5190.
[23] V. N. Knyukshto, K. N. Solovyov, G. D. Egorova, *Biospectroscopy* **1998**, *4*, 121-133.
[24] I. V. Avilov, A. Y. Panarin, V. S. Chirvony, *Chem. Phys. Lett.* **2004**, *389*, 352-358.
[25] F. Scandola, C. Chiorboli, A. Prodi, E. Iengo, E. Alessio, *Coord. Chem. Rev.* **2006**, *250*, 1471-1496.
[26] V. V. Borovkov, Y. Inoue, *Top. Curr. Chem.* **2006**, *265*, 89-146.
[27] G. A. Hembury, V. V. Borovkov, Y. Inoue, *Chem. Rev. (Washington, DC, U. S.)* **2008**, *108*, 1-73.
[28] L. Rosaria, A. D'Urso, A. Mammana, R. Purrello, *Chirality* **2008**, *20*, 411-419.
[29] N. Berova, L. Di Bari, G. Pescitelli, *Chem. Soc. Rev.* **2007**, *36*, 914-931.
[30] Y. Zhang, P. Chen, Y. Ma, S. He, M. Liu, *ACS Appl. Mater. Interfaces* **2009**, *1*, 2036-2043.
[31] K. S. Chan, X. Zhou, B. S. Luo, T. C. W. Mak, *J. Chem. Soc., Chem. Commun.* **1994**, 271-272.
[32] J.-Z. Zou, Z. Xu, M. Li, X.-Z. You, H.-Q. Wang, *Acta Crystallogr., Sect. C: Cryst. Struct. Commun.* **1995**, *C51*, 760-761.
[33] M. Gruden, S. Grubisic, A. G. Coutsolelos, S. R. Niketic, *J. Mol. Struct.* **2001**, *595*, 209-224.
[34] P. Bhyrappa, M. Nethaji, V. Krishnan, *Chem. Lett.* **1993**, 869-872.
[35] K. M. Kadish, M. M. Morrison, *J. Am. Chem. Soc.* **1976**, *98*, 3326-3328.
[36] K. M. Kadish, J. L. Cornillon, C. L. Yao, T. Malinski, G. Gritzner, *J. Electroanal. Chem. Interfacial Electrochem.* **1987**, *235*, 189-207.
[37] R. A. Ransdell, C. C. Wamser, *J. Phys. Chem.* **1992**, *96*, 10572-10575.
[38] R. C. Weast, in *Handbook of Chemistry and Physics- 66th Edition*, CRC Press, Boca Raton, Florida, **1985**, pp. E50-52.
[39] C. Reichardt, in *Solvents and Solvent Effects in Organic Chemistry*, Wiley-VCH, Weinheim, **2003**, pp. 23-26, 418-424.
[40] J. L. Sessler, D. Seidel, *Angew. Chem., Int. Ed.* **2003**, *42*, 5134-5175.
[41] L. Cuesta, E. Tomat, V. M. Lynch, J. L. Sessler, *Chem. Commun.* **2008**, 3744-3746.
[42] J. M. M. Rodrigues, A. S. F. Farinha, P. V. Muteto, S. M. Woranovicz-Barreira, F. A. Almeida Paz, M. G. P. M. S. Neves, J. A. S. Cavaleiro, A. C. Tome, M. T. S. R. Gomes, J. L. Sessler, J. P. C. Tome, *Chem. Commun.***2014**, *50*, 1359-1361.
[43] S. K. Kim, J. Lee, N. J. Williams, V. M. Lynch, B. P. Hay, B. A. Moyer, J. L. Sessler, *J. Am. Chem. Soc.* **2014**, *136*, 15079-15085.
[44] R. C. Jagessar, M. Shang, W. R. Scheidt, D. H. Burns, *J. Am. Chem. Soc.* **1998**, *120*, 11684-11692.
[45] Y.-H. Kim, J.-I. Hong, *Tetrahedron Lett.* **2000**, *41*, 4419-4423.
[46] P. D. Beer, M. G. B. Drew, R. Jagessar, *J. Chem. Soc., Dalton Trans.* **1997**, 881-886.
[47] C. Bucher, C. H. Devillers, J.-C. Moutet, J. Pecaut, J. L. Sessler, *Chem. Commun.***2006**, 3891-3893.
[48] O. Almarsson, A. Blasko, T. C. Bruice, *Tetrahedron* **1993**, *49*, 10239-10252.
[49] A. J. Bard, L. R. Faulkner, John Wiley & Sons, Inc., New York, **2001**, pp. 226-260.
[50] H. H. Thanga, A. L. Verma, *New J. Chem.* **2002**, *26*, 342-346.
[51] P. K. Kumar, P. Bhyrappa, B. Varghese, *Tetrahedron Lett.* **2003**, *44*, 4849-4851.
[52] T. Wijesekera, A. Matsumoto, D. Dolphin, D. Lexa, *Angew. Chem.* **1990**, *102*, 1073-1074.
[53] P. Bhyrappa, V. Krishnan, *Inorg. Chem.* **1991**, *30*, 239-245.
[54] C. H. Devillers, A. K. D. Dime, H. Cattey, D. Lucas, *C. R. Chim.* **2013**, *16*, 540-549.
[55] D. K. Dogutan, M. Ptaszek, J. S. Lindsey, *J. Org. Chem.* **2007**, *72*, 5008-5011.
[56] X. Q. Lin, K. M. Kadish, *Anal. Chem.* **1985**, *57*, 1498-1501.
[57] P. E. Ellis, Jr., J. E. Linard, T. Szymanski, R. D. Jones, J. R. Budge, F. Basolo, *J. Am. Chem. Soc.* **1980**, *102*, 1889-1896.
[58] D. Brault, M. Rougee, *Biochemistry* **1974**, *13*, 4591-4597.

FULL PAPER

The combined effects of solution conditions and macrocyclic structure determine the redox behavior of free-base porphyrins in acidic nonaqueous media. Each porphyrin undergoes two reductions at the π-ring system which occur in well-separated or overlapping electron transfer steps at potentials between 0.00 and -1.36 V vs SCE. Protonation constants were obtained and spectra of the electroreduced diprotic porphyrins were characterized byspectroelectrochemistry.

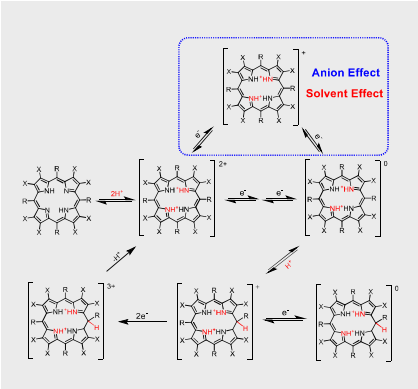

Y. Cui,[a] L. Zeng,[a] Y. Fang,[a] J. Zhu,[a]C. H. Devillers,[b] D. Lucas,[b] N. Desbois,[b] C. P. Gros,[b] Karl M. Kadish*[a]*

Page No. – Page No.

Tuning the Electrochemistry of Free-Base Porphyrins in Acidic Nonaqueous Media:Influence of Solvent, Supporting Electrolyte and RingSubstituents